Influence of 2-Aminopyridine on the Formation of Molybdates under Hydrothermal Conditions

Katikaneani Pavani[a] and Arunachalam Ramanan*[a]

Keywords: Hydrothermal synthesis / N ligands / Molybdenum / Crystal structure

The hydrothermal reaction of an aqueous ammonium heptamolybdate solution with first-row transition metal salts in the presence of 2-aminopyridine at around 180 °C and under autogenous pressure yields several molybdates, such as the 1D chains in $(C_5N_2H_7)_4Mo_8O_{26}$ (**1**), zero-dimensional $(C_5N_2H_7)_6Mo_7O_{24}\cdot 3H_2O$ (**2**), and the first synthesis of Lindgrenite $[Cu_3Mo_2O_8(OH)_2$ (**3**)] The structures of these materials were established by single-crystal and powder X-ray diffraction techniques. The crystal structures of wolframite-based $MnMoO_4$ (**4**) and $ZnMoO_4$ (**5**) were established by powder X-ray diffraction. The role of 2-aminopyridine (2-ampy) in the formation of the different solids under hydrothermal conditions is discussed.

Introduction

Molybdenum oxide based materials are of contemporary interest due to their promising applications in the area of catalysis, sorption, electrical conductivity, magnetism, photochemistry, sensors, and energy storage.[1–5] Among these, transition-metal-containing molybdates are attractive candidates due to their structural, electronic, and catalytic properties.[6–10] For example, β-$FeMoO_4$ and $Fe_2(MoO_4)_3$ have been employed in the synthesis of formaldehyde from methanol on a commercial scale, and Fe–Mo–O catalysts exhibit good activity for the oxidation of toluene to benzaldehyde.[11] In addition, it has been found that β-$FeMoO_4$ is a very good precursor of catalysts for hydrodesulfurization (HDS) processes,[12] and cobalt and nickel molybdates are important components of industrial catalysts for the partial oxidation of hydrocarbons and precursors in the synthesis of catalysts for hydrodesulfurization (HDS). Manganese- and nickel-containing molybdates are also potential electrode materials in rechargeable lithium batteries.[13] In recent times, soft chemistry routes, including hydrothermal reactions, have been commonly employed for the manipulation of hybrid molybdates in the presence of organic molecules as structure directors. The role of organic amines has been extensively investigated in the formation of discrete polyoxometalate clusters to three-dimensional networks of molybdenum oxide based materials.[14–20] It is well known that when polyoxomolybdate(POM)-based solids are crystallized from aqueous solution (either under ambient or hydrothermal conditions) in the presence of organic amines, organic/inorganic hybrid salts are invariably formed. These may be salts between organic cations and discrete polyoxomolybdate anions or composite solids with extended POM anions incorporated with organic cations. If an additional transition metal ion is present, the metal complex can either be present as a countercation or as part of the extended network linking POM cluster anions. An examination of the synthetic methodologies reported in the literature suggests that there have been very few attempts to rationalize the reactivity pattern in the formation of these solids. It is important to examine the role of organic amines in a systematic fashion to understand the critical issues involved in controlling the reaction and hence the structure of molybdates, even though hydrothermal reactions are commonly termed as "black-box" in nature. This paper is an attempt in this direction to identify the phases formed in the presence of an organic amine by employing identical reaction conditions and varying only the nature of the metal. We preferred the aromatic diamine 2-aminopyridine ($pK_a \approx 6.9$) as it forms weak complexes with transition metals and hence is readily labile in the presence of hydroxy ligands (Scheme 1) during hydrolysis and condensation reactions to produce an –M–O–Mo–O–M– network. Also, the amine has good solubility in aqueous solution and is hydrothermally stable. This paper describes the synthesis and characterization of several molybdates and proposes a rational model to explain the influence of 2-aminopyridine on their formation under hydrothermal conditions.

Results and Discussion

Powder X-ray diffraction analysis showed that single-phase crystalline molybdates were obtained only from the reactions containing manganese, cobalt, nickel, copper, or

[a] Department of Chemistry, Indian Institute of Technology, New Delhi 110016, India
Fax: +91-11-26582037
E-mail: aramanan@chemistry.iitd.ac.in

 DOI: 10.1002/ejic.200500092

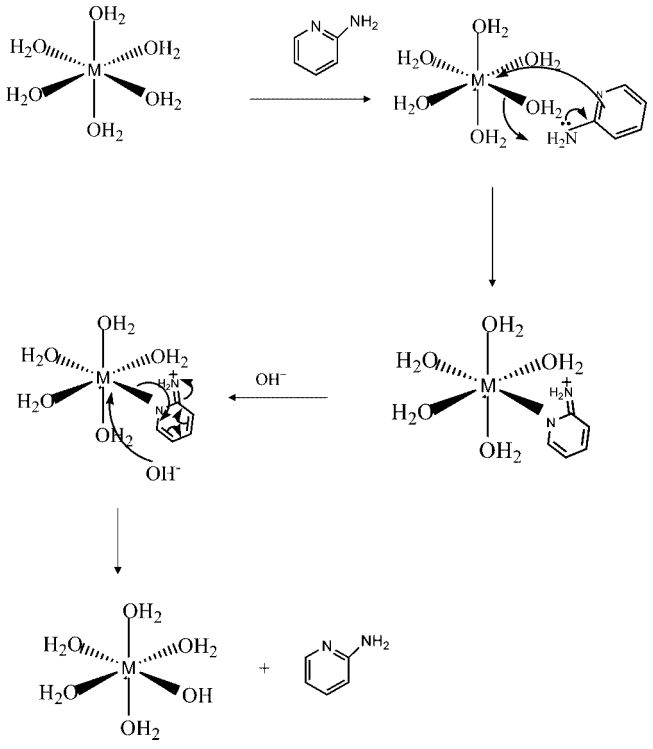

Scheme 1. Role of 2-ampy as a labile group in the hydrolysis condensation of a metal complex.

zinc. In the case of iron(II) chloride, hydrothermal treatment led to amorphous products. Table 1 lists the experimental conditions applied for the hydrothermal synthesis of molybdates, along with phase identification as established by powder and single-crystal X-ray diffraction. Scheme 2 shows the molybdates that were crystallized under hydrothermal conditions in the presence of 2-ampy. In all cases the yields were much higher than 70% (based on molybdenum) and the compounds were isolated as single phases, as determined by thermal studies and powder XRD. The powder X-ray diffraction patterns of $MnMoO_4$ (**4**) and $ZnMoO_4$ (**5**) are similar and the cell parameters and intensities correspond to the Wolframite structure reported in the literature.[21–23] In the case of cobalt and nickel, we obtained a polyoxometalate-based solid **2** that does not contain cobalt or nickel. Hydrothermal treatment of ammonium heptamolybdate and 2-ampy in the absence of a transition metal led to another new solid **1**. The crystal structures of solids **1** and **2** were further established by single-crystal X-ray diffraction. The hydrothermal reaction of ammonium molybdate solution with copper(II) ions in the presence of 2-ampy resulted in the formation of the pure Lindgrenite phase $Cu_3Mo_2O_8(OH)_2$ (**3**). Interestingly, this is the first laboratory synthesis and characterization of the mineral Lindgrenite. Both powder and single-crystal X-ray diffraction data of the product are consistent with the previously reported

Table 1. Experimental details.

Reactants, molar ratio, initial pH	Phase	Space group	Cell parameters	Colour/Morphology
$(NH_4)_6Mo_7O_{24}{\cdot}4H_2O$/2-ampy/$H_2O$, 1:12:1600, pH ≈ 6	$(C_5N_2H_7)_4Mo_8O_{26}$ (**1**) one-dimensional chains	$P2_1/c$ $Z = 2$	$a = 8.243(1)$ Å $b = 20.623(3)$ Å $c = 11.602(1)$ Å $\beta = 93.948(2)°$ $V = 1967.9(5)$ Å^3	White rods
$(NH_4)_6Mo_7O_{24}{\cdot}4H_2O$/$MnCl_2{\cdot}4H_2O$/2-ampy/$H_2O$, 1:8:12:1600, pH ≈ 6	$MnMoO_4$ (**4**) Wolframite	$P2/c$ $Z = 2$	$a = 4.8064$ (4) Å $b = 5.7482$ (4) Å $c = 4.9606$ (5) Å $\beta = 90.831(5)°$ $V = 137.7(1)$ Å^3	Brown rods
$(NH_4)_6Mo_7O_{24}{\cdot}4H_2O$/$Co(CH_3COO)_2{\cdot}6H_2O$ or $NiSO_4{\cdot}6H_2O$/2-ampy/H_2O, 1:8:12:1600, pH ≈ 6	$(C_5N_2H_7)_6Mo_7O_{24}{\cdot}3H_2O$ (**2**) zero-dimensional cluster	$P2_1/n$ $Z = 4$	$a = 14.828(1)$ Å $b = 17.5145(1)$ Å $c = 20.863(1)$ Å $\beta = 107.500(1)°$ $V = 5167.5(6)$ Å^3	Brown blocks
$(NH_4)_6Mo_7O_{24}{\cdot}4H_2O$/$CuCl_2{\cdot}2H_2O$/2-ampy/$H_2O$, 1:8:12:1600, pH ≈ 6	$Cu_3Mo_2O_8(OH)_2$ (**3**) Lindgrenite	$P2_1/n$ $Z = 2$	$a = 5.3928(9)$ Å $b = 14.022(2)$ Å $c = 5.607(1)$ Å $\beta = 98.473$ (3)° $V = 419.43(1)$ Å^3	Green rods
$(NH_4)_6Mo_7O_{24}{\cdot}4H_2O$/$CuCl_2{\cdot}2H_2O$/$H_2O$, 1:8:1600, pH ≈ 6	$(NH_4)_xMo_6O_{18}.yH_2O$ (**6**)	$P\bar{3}$ $Z = 1$	$a = 10.5388(7)$ Å $c = 3.7242(5)$ Å $V = 358.22(6)$ Å^3	White, hexagonal rods
$(NH_4)_6Mo_7O_{24}{\cdot}4H_2O$/$ZnSO_4{\cdot}7H_2O$/2-ampy/$H_2O$, 1:8:12:1600, pH ≈ 6	$ZnMoO_4$ (**5**) Wolframite	$P2/c$ $Z = 2$	$a = 4.668(5)()$ Å $b = 5.7194(6)$ Å $c = 4.8719(6)$ Å $\beta = 89.72(1)°$ $V = 130.07$ Å^3	Black blocks

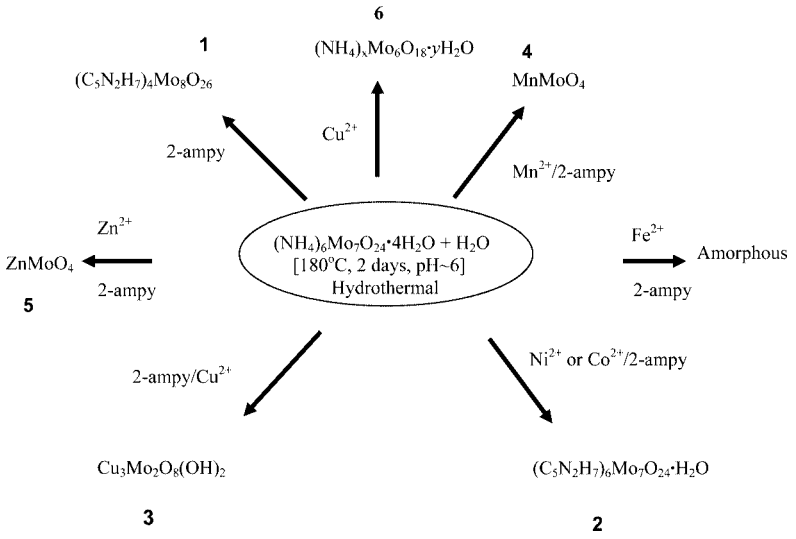

Scheme 2. Experimental details.

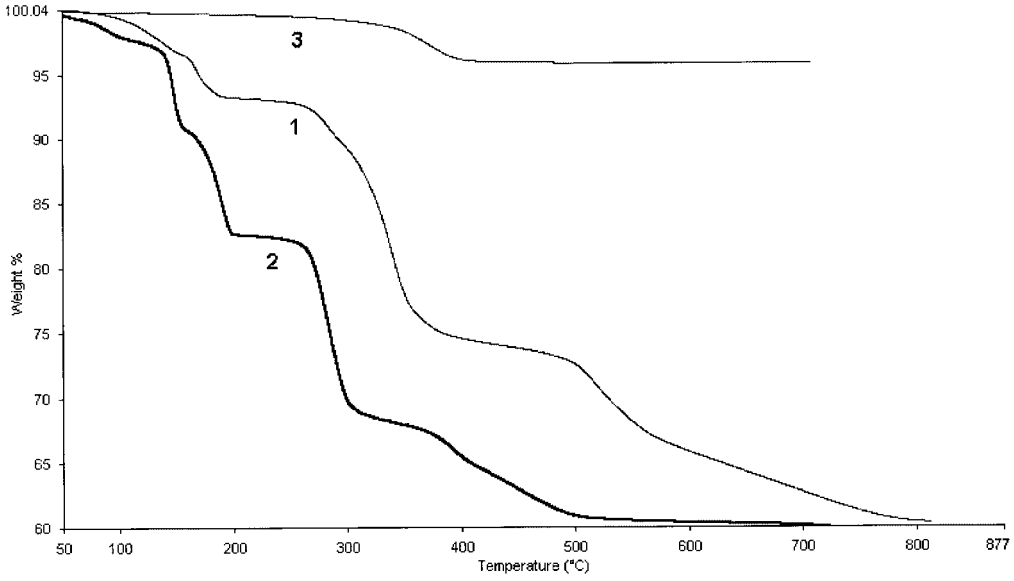

Figure 1. TGA data of compounds **1**–**3**.

crystal structure of the mineral.[24] This solid does not contain 2-ampy and, in its absence, the hydrothermal reaction yields the well-known hexagonal molybdate $(NH_4)_x$-$Mo_6O_{18}{\cdot}yH_2O$ (**6**).[25,26] However when the reaction was carried out with MoO_3 as a starting precursor it resulted in the formation of compound **2**, which is based on a heptamolybdate cluster**.** This indicates that the heptamolybdate phase is stable under these conditions. Thermal analysis of the solids was carried out under nitrogen (Figure 1). $MnMoO_4$(**4**) and $ZnMoO_4$(**5**) do not show any significant weight loss, thus confirming that they are anhydrous substances. In case of **3**, a broad weight loss in the temperature range 175–400 °C shows the loss of one water molecule to give a final composition of $Cu_3Mo_2O_9$. Both **1** and **2** lose their water molecules and organic groups in multiple steps. Weight loss up to 500 °C is probably due to the loss of water and organic groups and corresponds to the composition determined from single-crystal X-ray analysis.

Crystal Structure of 1

The crystal structure of **1** consists of 2-ampy cations and infinite anionic molybdenum oxide chains that are built from edge-sharing octamolybdate clusters $[Mo_8O_{28}]$ (Figure 2a). The $\{Mo_8O_{26}\}_\infty$ chains propagate along the *a*-axis (Figure 2d). Each chain is surrounded by six others (Figure 3). The interchain regions are filled with 2-ampy cations that participate in extensive, strong hydrogen bonding with cluster oxygen atoms. Each Mo_8O_{28} cluster is hydrogen-bonded to four 2-ampy cations through the terminal oxygen atoms O3 and O10 of the cluster. The crystal data are pro-

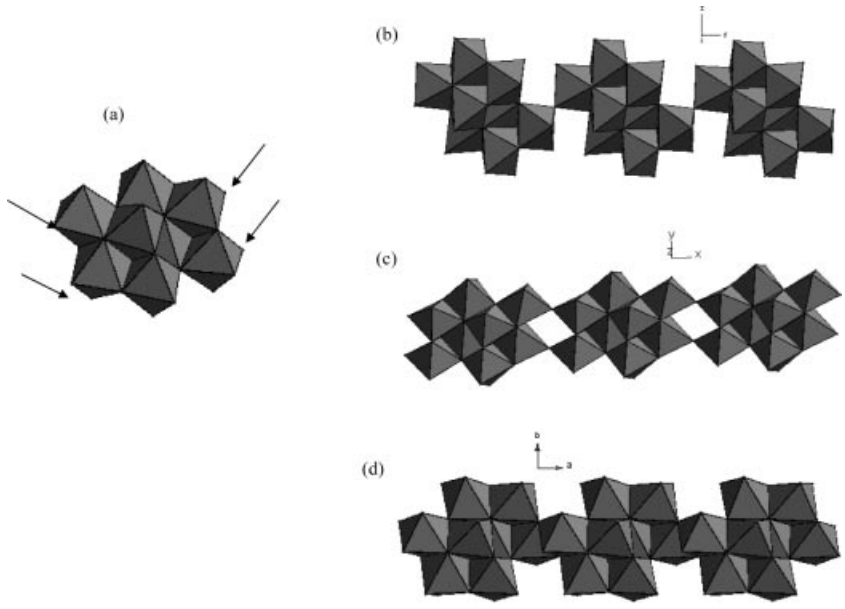

Figure 2. (a) Polyhedral representation of the octamolybdate. Sites through which the subunits are linked into infinite chains in **1** are denoted with arrows. (b) The linkage of octamolybdates through common corners to form chains with the $(Mo_8O_{27})_n^{6n-}$ composition. (c) The linkage of octamolybdates is through pairs of Mo–O–Mo bridges to form a molybdenum oxide chain with the $(Mo_8O_{26})_n^{4n-}$ composition. (d) The linkage of octamolybdates through common edges to form chains with the $(Mo_8O_{26})_n^{4n-}$ composition as in the case of **1**.

vided in Table 2. The Mo–O distances are significantly different due to multiple bonding character and range from 1.687(3) to 2.504 (3) Å. The octamolybdate chains found in **1** are similar to those in two other tetramolybdates, namely $K_2Mo_4O_{13}$[27] and $(NH_4)_2Mo_4O_{13}$.[28] Two other octamolybdates with a slightly different composition, namely $(NH_4)_6Mo_8O_{27}\cdot 4H_2O$ and $(C_4H_{12}N_2)_3Mo_8O_{27}$ ($C_4H_{12}N_2$ = piperazinium ion),[29] and a polymeric octamolybdate [$(MeNC_5H_5)_4Mo_8O_{26}$] reported by Zubieta et al.[30] are also known. The composition of the polymeric solid depends upon the connectivity pattern between the basic octamolybdate fragments. In $(MeNC_5H_5)_4Mo_8O_{26}$, the octamolybdate subunits are connected by linear and symmetrical Mo–O–Mo bridges into infinite chains (Figure 2c), while in $(NH_4)_6Mo_8O_{27}\cdot 4H_2O$ and $(C_4H_{12}N_2)_3Mo_8O_{27}$, the octamolybdate subunits share common corners (Figure 2b). The linkage of octamolybdate blocks through common edges, i.e., the connectivity mode encountered in $(C_5N_2H_7)_4[Mo_8O_{26}]$ (**1**), again results in an $[Mo_8O_{26}]^{4-}$ stoichiometry for the chains (Figure 2d).

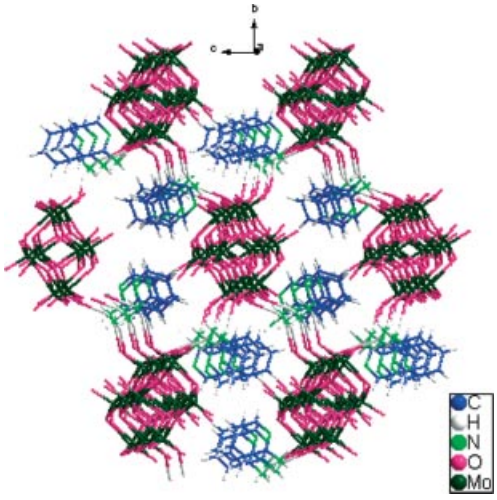

Figure 3. Projection of the unit cell of **1** along the *a*-axis showing the H-bonding between the octamolybdate chain and 2-aminopyridine.

Table 2. Crystal data of compounds **1**–**3**.

Empirical formula	**1**	**2**	**3**
Crystal system	monoclinic	monoclinic	monoclinic
Space group	$P2_1/c$	$P2_1/n$	$P2_1/n$
T [K]	300(2)	300(2)	300(2)
a [Å]	8.243(1)	14.8280(10)	5.3928(9)
b [Å]	20.623(3)	17.5145(12)	14.023(2)
c [Å]	11.602(1)	20.8632(14)	5.6076(10)
α [°]	90	90	90
β [°]	93.94	107.5	98.473
γ [°]	90	90	90
V [Å^3]	1967.9(5)	5167.5(6)	419.43(13)
Z	2	4	2
Collected reflections	16770	58670	4313
Unique reflections	4618	12265	988
Observed reflections	4431	11149	984
R [$I > 2\sigma(I)$]	0.0227	0.032	0.0467
wR_2 (all)	0.06042	0.0957	0.1271

Crystal Structure of 2

The crystal structure of $(C_5N_2H_7)_6Mo_7O_{24}\cdot 3H_2O$ (**2**) is that of a heptamolybdate $[Mo_7O_{24}]^{6-}$ based solid. The Mo_7O_{24} cluster anion contains a central $\{Mo_3O_8\}$ core

built of three edge-shared MoO_6 octahedral units arranged in a 1×3 rectangular array; two MoO_6 units from above and two from below share the equatorial oxygen atoms at the apices of the octahedra in the rectangle. Each Mo^{VI} atom in the Mo_7O_{24} cluster has a distorted octahedral geometry with an Mo–O bond length in the range of 1.702(3)–2.298(2) Å for terminal and bridging oxygen atoms. Each $Mo_7O_{24}^{6-}$ anion is surrounded by six 2-ampy cations (Figure 4). Each cluster anion exhibits strong H-bonding with six of the 2-ampy cations and only terminal oxygen atoms participate in this H-bonding. Although all six 2-ampy cations are involved in H-bonding, only two of them connect the clusters into an extended 1D chain (Figure 5). The water molecules present also form strong H-bonds among themselves as well as with cluster oxygen atoms. This solid is identical to that reported in the literature, except that we have grown it under hydrothermal conditions.[31] All the bond angles and distances are consistent with Mo_7O_{24} clusters observed in previous reports.[32–34]

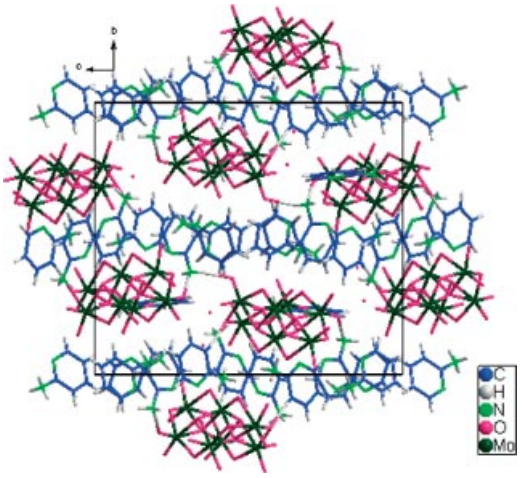

Figure 4. $\{Mo_7O_{24}\}^{6-}$ cluster anions exhibiting H-bonding with water and 2-aminopyridinium cations in **2**.

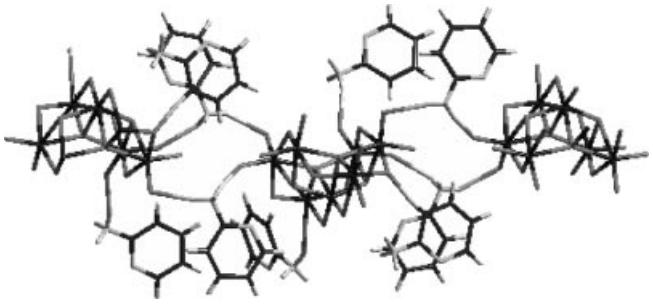

Figure 5. View showing the infinite 1D chain formation of $\{Mo_7O_{24}\}^{6-}$ clusters via the strong H-bonding with 2-aminopyridium cations in **2**.

Crystal Structure of 3

The single-crystal structural analysis of **3** is very similar to that of the naturally occurring mineral Lindgrenite solved by Hawthorne et al.[24] The vanadium analog of **3** has also been reported recently.[35] There are two asymmetric copper atoms in the crystal structure of the synthetic analog of Lindgrenite $[Cu_3Mo_2O_8(OH)_2]$, one of which occurs at the special position, as well as one asymmetric molybdenum and five asymmetric oxygen atoms which all occupy the general position (4e). While the molybdenum atoms are coordinated by four oxygen atoms in a pseudo-tetrahedral arrangement, the copper atoms are pseudo-octahedrally coordinated by oxygen atoms. There is a strong Jahn–Teller distortion around both copper centers, with considerable extension of the apical bonds when compared with the equatorial bonds. The two hydrogen atoms are bonded to O1 and O4. A prominent feature of the Lindgrenite structure is the strips of edge-sharing CuO_6 octahedra that run parallel to the *c*-axis (Figure 6). These strips are cross-linked by MoO_4 tetrahedra that share corners with the CuO_6 octahedra; each MoO_4 tetrahedron links three strips together, with the fourth linkage occurring along the length of one of the strips (Figure 7).

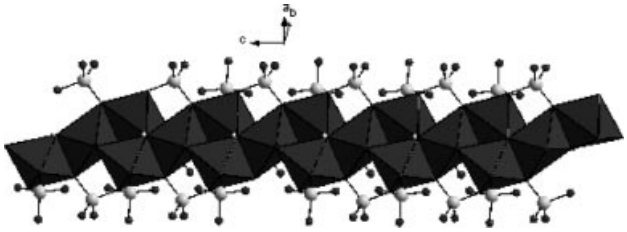

Figure 6. Strips of edge-sharing CuO_6 octahedra running parallel to the *c*-axis in **3**.

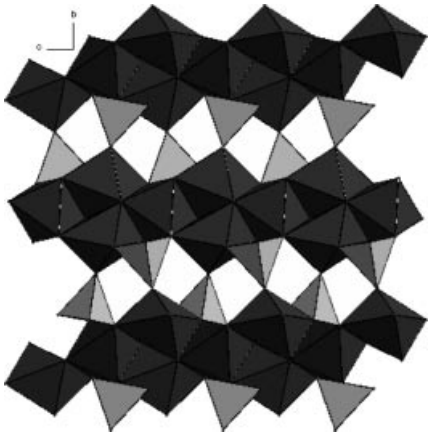

Figure 7. Crystal structure of Lindgrenite (**3**) viewed along the *c*-axis.

Crystal Structures of 4 and 5

The powder X-ray diffraction patterns of $MnMoO_4$ (**4**) and $ZnMoO_4$ (**5**) are isostructural and suggest a Wolframite structure based on the cell parameters and intensities. We did not succeed in obtaining suitable single crystals under our reaction conditions. Both the molybdenum and manganese or zinc atoms in the Wolframite structure are octahedrally coordinated. Each octahedron has two short, two

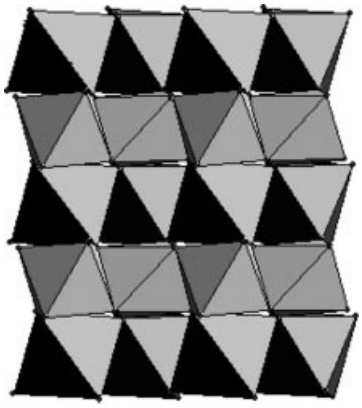

Figure 8. Crystal structural of $MMoO_4$ (M = Mn and Zn).

medium, and two long metal–oxygen bonds (Figure 8). The metal atoms occupy special positions while the oxygen atoms are at general positions. The octahedra are highly distorted with angles ranging from 72.9 (1) to 101.7 (1)° in the molybdenum-containing octahedron and from 75.7(1) to 110.6(2)° in the manganese one. Compounds **4** and **5** have also been synthesized earlier by other groups.[21–23] To the best of our knowledge, however, this is the first report of a low-temperature hydrothermal method for the synthesis of $MnMoO_4$ and $ZnMoO_4$.

Chemistry of the Formation of Molybdates by Hydrothermal Treatment

When heptamolybdates are dissolved in aqueous solution in the presence of 2-ampy (pH ≈ 6.0), other molybdate species such as $[MoO_3(OH)]^-$, $MoO_2(OH)_2(H_2O)_2$, $[Mo_8O_{26}]^{4-}$, and $[H_2Mo_8O_{28}]^{6-}$ may form due to a slight change in the pH and ionic strength of the medium, although heptamolybdate is the predominant cluster at equilibrium. The equilibrium species will change considerably when the aqueous molybdate solution is subjected to hydrothermal treatment.

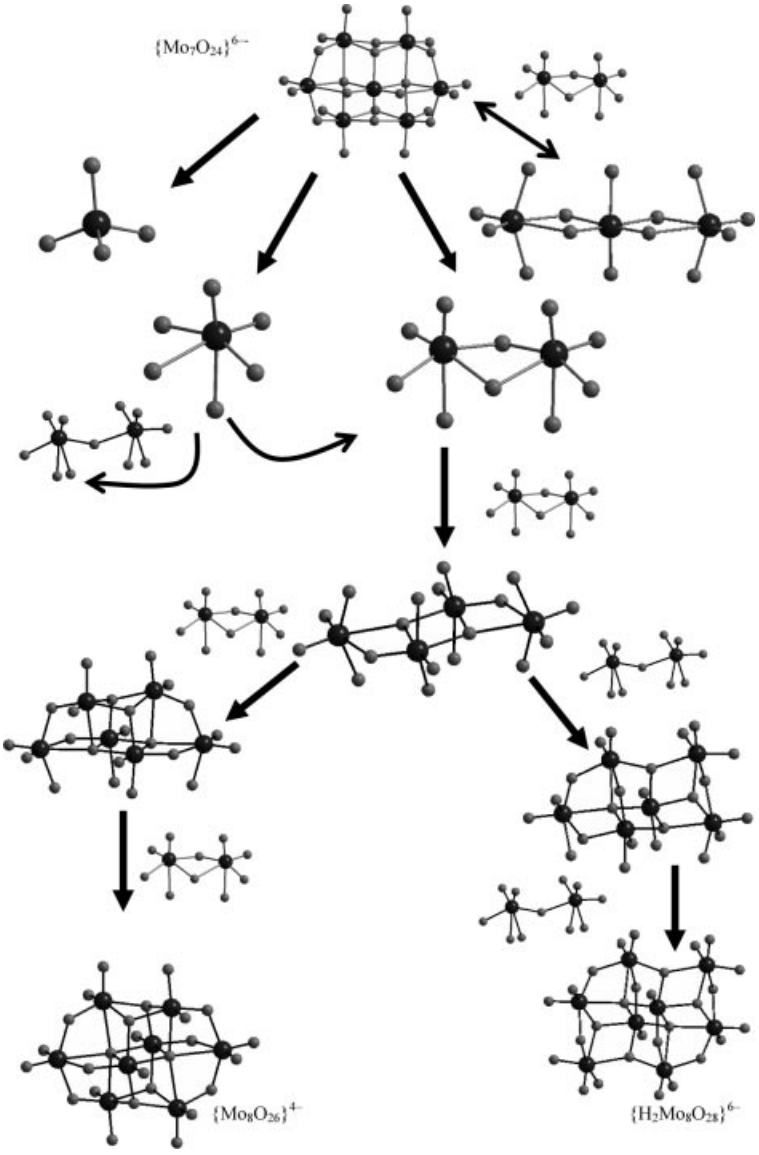

Figure 9. Hypothetical pathway for the self-assembly of polyoxomolybdate cluster anions from heptamolybdates.

Under these conditions, crystallization of a salt or a solid will be dominated by the electrostatic interactions between the polyoxomolybdate anions and the organic cations; secondary interactions taking place between the hydrated metal ions and other minor molybdate cluster anions, along with noncovalent interactions such as hydrogen bonding, may also influence the structure. On the basis of the solids obtained in this study, it is reasonable to assume that the heptamolybdate cluster anion dominates the equilibrium as long as the reaction is carried out under self-assembly conditions at room temperature without the addition of acid or hydrothermal treatment. In addition, other metal ions in the medium (such as cobalt or nickel) do not compete with the organic ligand (2-ampy in our case). As the larger anion prefers a larger cation, we invariably obtain a salt based on heptamolybdate $[Mo_7O_{24}]^{6-}$ along with the organic cation as in **2**. Since heptamolybdates are hardly protonated, the packing of the final solids is influenced by the hydrogen-bonding interaction between the anions, cations and water molecules, as demonstrated in the structure of **2**. The presence of weakly acidic cobalt or nickel hydrates is responsible for keeping the heptamolybdate clusters stable in solution. The reaction carried out in the absence of these metal ions results in the formation of **1**. Under slightly acidic conditions, the heptamolybdate undergoes fragmentation into smaller units, including MoO_4 and MoO_6 units. A few of these smaller fragments of oxomolybdenum clusters can reassemble to form larger clusters such as $[Mo_8O_{26}]^{4-}$, $[H_2Mo_8O_{28}]^{6-}$, etc. (Figure 9). The cluster $[H_2Mo_8O_{28}]^{6-}$, with its large negative charge, is not completely stable in aqueous solution and under hydrothermal conditions tends to condense to form 1D polymeric chains of the composition $[Mo_8O_{26}]^{4-}{}_\infty$; in the presence of 2-ampy, the solid **1** crystallizes out. A similar framework is also known with K^+ and NH_4^+ cations. When we carried out a hydrothermal reaction of MoO_3 rather than ammonium heptamolybdate with 2-ampy, we obtained only the heptamolybdate cluster based solid **2**. Incidentally, **2** was also obtained when a hydrothermal reaction was carried out in the presence of nickel and cobalt ions. This suggests that the formation of POM clusters such as $[H_2Mo_8O_{28}]^{6-}$ and $[Mo_7O_{24}]^{6-}$ depends on the nature of the starting molybdenum precursor. The reactions occurring in the presence of manganese, copper, and zinc favor a shift in equilibrium towards MoO_x^{n-} species. In the case of Mn and Zn, a Wolframite-based $MMoO_4$ structure is stabilized. Unlike other metal ions, copper(II) ions tend to form polymeric chains[36–38] at around this pH, and these readily react with MoO_4^{2-} ions to give Lindgrenite (**3**). However, hydrothermal treatment of ammonium heptamolybdate with copper(II) ions in the absence of 2-ampy results in ammonium-intercalated hexagonal molybdates. We have previously shown that hexagonal molybdates are the most stable phases formed under hydrothermal conditions in the presence of monovalent alkali metal or ammonium ions.[26] Since we also obtained the Lindgrenite phase from the hydrothermal reaction of sodium molybdate and copper chloride solution (pH ≈ 6), 2-ampy provides a suitable pH for the fragmentation of heptamolybdates into tetrahedral MoO_4. The results reported here suggest that 2-ampy has a major influence on the formation of transition metal molybdates.

Conclusions

The hydrothermal reaction of aqueous ammonium heptamolybdate with manganese, cobalt, nickel, copper, or zinc ions in the presence of 2-aminopyridine results in the formation of several crystalline molybdates. A weak base such as 2-aminopyridine can act as a buffer and form weaker complexes with the transition metal, thus preventing its hydrolysis in aqueous solution. The hydrothermal medium can further influence the condensation of the protonated oxomolybdate clusters or the formation of metal molybdates.

Experimental Section

Syntheses: All chemicals were obtained from Aldrich and used without further purification. $(NH_4)_6Mo_7O_{24}{\cdot}4H_2O$ (0.625 mmol) was mixed with an appropriate amount of transition metal M^{2+} salts (M = Mn, Fe, Co, Ni, Cu, Zn; 5 mmol) and 2-ampy (7.5 mmol) in 18 mL of distilled water (1000 mmol). In order to rationalize the influence of 2-ampy, we also carried out a blank reaction as above without the transition metal chloride. The mixture was transferred into a 30-mL Teflon-lined acid digestion reactor and heated at 180 °C for 2 d and then cooled slowly to room temperature. The pH of the reaction before and after was found to be about 6 in all cases. To investigate the influence of 2-ampy when the molybdenum source is MoO_3, the reaction was carried out by heating the mixture of MoO_3 and 2-ampy in the molar ratio 1:1.5 under the same conditions. In all the cases, the products were washed with water and dried in air at room temperature. All the solids were analyzed by powder X-ray diffraction (Bruker AXS diffractometer with Cu-K_α radiation) for crystallinity and phase identification. TG analyses were carried out with a Perkin–Elmer TGA7 system on well-ground samples under a nitrogen flow with a heating rate of 10 °C min^{-1}. In all cases the phase purity of the samples was established by simulating powder X-ray diffraction patterns on the basis of the single-crystal structure data.

X-ray Crystallography: Single-crystal diffraction studies were carried out with a Bruker SMART CCD diffractometer with Mo-K_α (λ = 0.71073Å) radiation at 28 °C for **1**–**3**. Table 1 lists the experimental parameters used for the single-crystal structure analyses. The software SADABS was used for absorption correction and SHELXTL for space-group and structure determination and refinements.[39,40] The molybdenum atoms were located first and then the remaining atoms were deduced from subsequent difference Fourier syntheses. The hydrogen atoms were located using geometrical constraints. All the atoms except H were refined anisotropically. Least-squares refinement cycles on F^2 were performed until the model converged. Experimental and crystal data are provided in Tables 1 and 2, respectively. CCDC-245096 (**1**) and -249182 (**2**) contain the supplementary crystallographic data for this paper. These data can be obtained free of charge from The Cambridge Crystallographic Data Centre via www.ccdc.cam.ac.uk/data_request/cif. Further details of the crystal-structure investigation for **3** may be obtained from the Fachinformationzentrum Karlsruhe, 76344 Eggenstein-Leopoldshafen, Germany, on quoting the depository number ICSD-415059.

Acknowledgments

K. P. thanks the CSIR for a research fellowship and A. R. acknowledges the DST, Government of India, for financial support. We thank Dr. N. G. Ramesh for helpful discussions. A. R. also thanks the DST for funding a powder X-ray diffractometer under IRHPA and a Smart Apex CCD single-crystal X-ray diffractometer under FIST for the Department of Chemistry at IIT, Delhi.

[1] A. M. Chippindale, A. K. Cheetham, in: *Studies in Inorgonic Chemistry*, Elsevier, Amsterdam, **1994**, vol. 19, p. 146–184, and references cited therein.
[2] L. F. Johnson, G. D. Boyd, K. Nassau, R. R. Soden, *Phys. Rev.* **1962**, *126*, 1406.
[3] D. W. Bruce, D. O.Hare, *Inorganic Materials*, Wiley, Chichester, **1992**.
[4] T. Bein, "Supramolecular Architecture", *ACS Symp. Ser.* **1992**, p. 499.
[5] A. K. Cheetham, *Science* **1994**, *264*, 794, and references cited therein.
[6] S. Soo Kim, S. Ogura, H. Ikuta, Y. Uchimoto, M. Wakihara, *Solid State Ionics* **2002**, *146*, 249–256.
[7] J. L. Brito, A. L. Barbosa, *J. Catal.* **1997**, *171*, 467–475.
[8] J. Miller, A. G. Sault, N. B. Jackson, L. Evans, M. Gonzales, *Catal. Lett.* **1999**, *58*, 147–152.
[9] L. M. Madeira, M. F. Portela, C. Mazzochia, A. Kaddouri, R. Anouchinsky, *Catal. Today* **1998**, *40*, 229–243.
[10] G. E. Vrieland, C. B. Murchison, *Appl. Catal. A* **1996**, *134*, 101–121.
[11] H. Zhang, J. Shen, X. Ge, *J. Solid State Chem.* **1995**, *117*, 127–135.
[12] J. A. Rodriguez, J. C. Hanson, S. Chaturvedi, A. Maiti, J. L. Brito, *J. Phys. Chem. B* **2000**, *104*, 8145–8152.
[13] Y. Idemoto, H. Sekine, K. Ui, N. Koura, *Solid State Ionics* **2005**, *176*, 299–306.
[14] A. Briceno, R. Atencio, *Acta Crystallogr., Sect. E* **2004**, *60*, i47–i49.
[15] J. B. Strong, G. P. A. Yap, R. Ostrander, L. M. Liable-Sands, A. L. Rheingold, R. Thouvenot, P. Gouzerh, E. A. Maatta, *J. Am. Chem. Soc.* **2000**, *122*, 639–649.
[16] D. G. Allis, R. S. Rarig, E. Burkholder, J. Zubieta, *J. Mol. Struct.* **2004**, *688*, 11–31.
[17] P. J. Hagrman, D. Hagrman, J. Zubieta, *Angew. Chem. Int. Ed.* **1999**, *38*, 2639–2684.
[18] P. Q. Zheng, Y. P. Ren, L. S. Long, R. B. Huang, L. S. Zheng, *Inorg. Chem.* **2005**, *44*, 1190–1192.
[19] T. Duraisamy, A. Ramanan, J. J. Vittal, *J. Mater. Chem.* **1999**, *9*, 763–767.
[20] S. Upreti, A. Ramanan, *Inorg. Chim. Acta* **2005**, *358*, 1241–1246.
[21] A. W. Sleight, B. L. Chamberland, *Inorg. Chem.* **1968**, *7*, 1672–1675.
[22] A. P. Young, C. M. Schwartz, *Science* **1963**, *141*, 348–349.
[23] A. Clearfield, A. Moini, P. R. Rudolf, *Inorg. Chem.* **1985**, *24*, 4606–4609.
[24] F. C. Hawthorne, R. K. Eby, *Neues Jahrb. Mineral., Monatsh.* **1985**, *5*, 234–240.
[25] N. Sotani, *Bull. Chem. Soc. Jpn.* **1975**, *48*, 1820–1825.
[26] S. Upreti, A. Ramanan, *Proc. Indian Acad. Sci. (Chem. Sci.)* **2003**, *115*, 411–417.
[27] B. M. Gatehouse, P. Leverette, *J. Chem. Soc., A* **1971**, 2107–2112.
[28] R. Benchrifa, M. Leblanc, R. de Pape, *Eur. J. Solid State Inorg. Chem.* **1989**, *26*, 593–601.
[29] W. T. A. Harrison, L. L. Dussack, A. J. Jacobson, *Acta Crystallogr., Sect. C* **1996**, *52*, 1075–1077.
[30] B. Modec, J. V. Brencic, J. Zubieta, *Inorg. Chem. Commun.* **2003**, *6*, 506–512.
[31] P. Roman, J. M. Gutierrez Zorrilla, R. M. Martinez, S. G. Blanco, *Transition Met. Chem.* **1986**, *11*, 143–150.
[32] Z. Han, H. Ma, J. Peng, Y. Chen, E. Wang, N. Hu, *Inorg. Chem. Commun.* **2004**, *7*, 182–185.
[33] H. A. Hashmi, *Solid State Ionics* **1997**, *96*, 209–214.
[34] P. Gili, P. A. Lorenzo Luis, A. Mederos, J. M. Arrieta, G. Germain, A. Castineiras, R. Carballo, *Inorg. Chim. Acta* **1996**, *295*, 106–114.
[35] C. D. Wu, C. Z. Lu, H. H. Zhuang, J. S. Huang, *Eur. J. Inorg. Chem.* **2003**, 2867–2871.
[36] S. Vilminot, M. R. Plouet, G. Andre, D. Swierezynski, M. Guillot, F. B. Vigneron, M. Drillon, *J. Solid State Chem.* **2003**, *170*, 255–264.
[37] R. Baies, V. Caignaert, V. Pralong, B. Raveau, *Inorg. Chem.* **2005**, *44*, 2376–2380.
[38] Y. Xu, J. Lu, N. K. Goh, *J. Mater. Chem.* **1999**, *9*, 1599–1602.
[39] G. M. Sheldrick, *Acta Crystallogr., Sect. A* **1990**, *46*, 467–473.
[40] G. M. Sheldrick, *SHELXTL-NT2000*, version 6.12, reference manual, University of Göttingen, Germany.

Received: January 28, 2005
Published Online: July 4, 2005

